Kinetics and Thermodynamics of CO Binding to Cytochrome $P450_{nor}$†

Yoshitsugu Shiro,*,‡ Minoru Kato,‡ Tetsutaro Iizuka,‡ Kazuhiko Nakahara,§ and Hirofumi Shoun§

Institute of Physical and Chemical Research (RIKEN), Wako, Saitama 351-01, Japan, and Institute of Applied Biochemistry, University of Tsukuba, Tsukuba, Ibaraki 305, Japan

Received January 31, 1994; Revised Manuscript Received May 11, 1994®

ABSTRACT: The CO-binding reaction of cytochrome $P450_{nor}$ isolated from denitrifying fungus, *Fusarium oxysporum*, has been studied by using a flash photolysis method in the millisecond time domain. We obtained the CO on- and off-rate constants in the bimolecular reaction, and determined the activation free energy, enthalpy, and entropy from the temperature dependence of these rate constants. To discuss the structural characteristics of $P450_{nor}$, these parameters were compared with those of other cytochrome P450s, such as cytochrome $P450_{cam}$ from *Pseudomonas putida* and myoglobin. The on-rate constant (k_{on}) for $P450_{nor}$ is larger than those of camphor-bound $P450_{cam}$ [$P450_{cam}(+)$], suggesting that ligand entry to the heme pocket of $P450_{nor}$ is sterically less restricted than that of $P450_{cam}(+)$. In the $P450_{nor}CO$ complex, the IR stretching band of the iron-bound CO is observed at 1942 cm^{-1}, which is the same position as in $P450_{cam}(+)CO$. This result suggests that the heme pocket immediate to the ligand-binding site is the same size in the two enzymes, in good agreement with the observation that the equilibrium constant ($K = k_{on}/k_{off}$) is identical in $P450_{nor}$ and $P450_{cam}(+)$. On the other hand, the entropy changes in the equilibrium and the off-activation processes are smaller in $P450_{nor}$ than in $P450_{cam}(+)$. This feature could reflect the lack of a bound substrate at the active site of $P450_{nor}$. These structural characteristics of $P450_{nor}$ are discussed in relation to its unique catalytic property, rapid NO reduction to yield N_2O.

Cytochrome P450 includes a number of *b*-type hemoproteins that have a characteristic electronic absorption band at 450 nm when combined with CO in the reduced (Fe^{2+}) state (Omura & Sato, 1962). The heme–enzyme catalyzes monooxygenation reactions, where one atom of molecular oxygen (O_2) is incorporated into a wide variety of hydrophobic substances. More than 100 species of cytochrome P450 have been identified as distinct entities. Of these, the most extensively studied is cytochrome $P450_{cam}$,[1] which is isolated from the bacterium *Pseudomonas putida* (Gunsalus et al., 1974; Sligar & Murray, 1986). $P450_{cam}$[1] catalyzes the monooxygenation reaction of *d*-camphor to yield 5-*exo*-hydroxycamphor, in which electrons are transferred from NADH through two redox-enzymes, putidaredoxin (an iron–sulfur protein) and its reductase (flavoprotein). Crystallographic studies of $P450_{cam}$ in several oxidation/spin/ligation states (Poulos et al., 1985, 1986, 1987; Poulos & Howard, 1987; Raag & Poulos, 1989a,b) have shown that the substrate camphor binds to the protein moiety of the heme distal side, which is close enough to the O_2-binding site. It is also revealed that the bound camphor sterically interacts with the iron-bound CO, which is an analog of the iron-bound O_2. Thus, during the catalytic reaction, where $P450_{cam}$ forms a ternary complex with *d*-camphor and O_2, the binding of the substrate and the binding of O_2 to the iron influence each other.

Recently, Shoun and his co-workers isolated and purified cytochrome $P450_{nor}$ from the denitrifying fungus *Fusarium oxysporum*, which is grown in the presence of nitrate or nitrite salts (Shoun et al., 1983, 1989; Shoun & Tanimoto, 1991). Compared with the usual P450s such as $P450_{cam}$, $P450_{nor}$ is very unique in its function, because it catalyzes the reduction of NO to N_2O by directly accepting electrons from NADH (Nakahara et al., 1993) but does not exhibit monooxygenase activity. These results allowed us to consider that $P450_{nor}$ does not have any hydrophobic substrate-binding site at its active site. In the hypothetical mechanism proposed, NO binds to Fe^{3+}, the resultant Fe^{3+}–NO moiety is directly reduced by NADH to yield Fe^{2+}–NO, followed by internal electron transfer to form Fe^{3+}–NO^-, and then NO^- is released. The resultant NO^- is nonenzymatically coupled, and N_2O is generated. Thus, the overall reaction catalyzed by $P450_{nor}$ is

$$2NO + 2e^- + 2H^+ \rightarrow N_2O + H_2O \qquad (1)$$

The amino acid sequence of $P450_{nor}$ deduced from its cDNA analysis (Kizawa et al., 1991) showed about 25% identity with that of $P450_{cam}$ and about 40% identity with that of *Streptomyces* $P450_{SU2}$, but the structures at the heme-binding domain and at the heme axial sites are highly homologous. Some spectral properties of $P450_{nor}$ are very similar to the corresponding ones of other P450s; e.g., the Soret absorption of its CO complex is located at 450 nm, and its ferric form shows ESR absorptions at $g = 8$ and 4. These studies have implied that the structure of $P450_{nor}$, at least at the heme vicinity, is probably similar to that of $P450_{cam}$. However, we cannot explain the unique catalytic function of $P450_{nor}$ in terms of its structural information accumulated so far.

To gain further insight into the structural characteristics of $P450_{nor}$, we examined here the CO-binding reaction. We carried out the kinetic measurements for the bimolecular CO-binding reaction (eq 2) at various temperatures and obtained several thermodynamic parameters (ΔG, ΔS, and ΔH) for the equilibrium, the *on*- and the *off*-activation processes.

† This work was supported by the Biodesign Research Program from RIKEN (to Y.S.), by the system of Special Researchers' Basic Science Program (to M.K.), and by Special Coordination Funds from the Science and Technology Agency of Japan.

* To whom correspondence should be addressed.

‡ Institute of Physical and Chemical Research (RIKEN).

§ University of Tsukuba.

® Abstract published in *Advance ACS Abstracts,* July 1, 1994.

[1] Abbreviations: $P450_{nor}$, cytochrome P450 isolated from *Fusarium oxysporum*; $P450_{cam}$, cytochrome P450 isolated from *Pseudomonas putida*; $P450_{cam}(+)$, *d*-camphor-bound form of cytochrome $P450_{cam}$; $P450_{cam}(-)$, *d*-camphor-free form of cytochrome $P450_{cam}$; Mb, myoglobin.

0006-2960/94/0433-8673$04.50/0

$$\text{P450} + \text{CO} \underset{k_{off}}{\overset{k_{on}}{\rightleftharpoons}} \text{P450CO} \qquad (2)$$

In addition to the kinetic and the thermodynamic studies, we also examined the IR spectra for the CO complex of $P450_{nor}$. These results obtained here reflect the structural characteristics or the conformational dynamics in the ligand (CO)-binding reaction, which possibly correlate to the catalytic function of $P450_{nor}$. In this study, we compare the kinetic, the thermodynamic, and the IR features of $P450_{nor}$ with the corresponding ones of $P450_{cam}$ and discuss them in relation to differences in their functions.

MATERIALS AND METHODS

Enzymes. Cytochrome $P450_{nor}$ was isolated from *Fusarium oxysporum* (MT-811), which was purified by column chromatographies as described elsewhere (Nakahara et al., 1993). Cytochrome $P450_{cam}$ was kindly donated by Prof. R. Makino of the Himeji Institute of Technology. The protein solutions were concentrated to about 1 mM with a DIAFLO membrane (Amicon) as stock protein samples. For the preparation of the CO complexes, each degassed ferric cytochrome P450 solution was reduced with a small amount of sodium dithionite and equilibrated with a gas mixture of CO and N_2. The concentration (30–125 μM) of the CO solution at a known temperature, which was regulated by a gas divider (Estec Model SGD-XC-0.5L), was determined using Henry's law.

Flash Photolysis Measurements. The protein concentration for the flash photolysis experiment was about 4 μM. The buffer used was 0.1 M potassium phosphate at pH 7.2. The temperature of the sample was controlled within an error of ±0.2 °C by circulating thermostated water around the cell. The CO-binding rates of cytochrome $P450_{cam}$ and $P450_{nor}$ were measured with a UNISOKU laser photolysis spectrometer equipped with a flash lamp pumped dye laser showing a duration of 300 ns (UNISOKU LA-501) (Sato et al., 1990a,b). Rhodamine 6G (Wako) in methanol was used to produce an excitation flash at a wavelength of 590 nm. The probe light at 448 nm was monitored by a monochromator (UNISOKU USP-501) with a photomultiplier. The time course measurements were recorded not more than 10 times at each temperature. Before and after the laser exposure, the sample was checked by the visible absorption spectrum (Hitachi U-3210).

IR Measurement. The IR spectrum of the CO complex of $P450_{nor}$ was measured by using a JEOL JIR 6500 with a resolution of 2 cm^{-1} at room temperature. The sample for the IR measurement, whose concentration was 1 mM, was transferred into the IR cell with CaF_2 windows (path length, 0.050 mm).

RESULTS

Figure 1 shows the difference spectral change in the CO complex of $P450_{nor}$ after the laser irradiation. The spectra after photolyzing the bound CO were exactly the same as the difference spectrum of the CO-free minus -bound forms of $P450_{nor}$. Detection of isosbestic points in this spectral change was indicative of no intermediate in the CO rebinding to ferrous $P450_{nor}$ on this time scale. We then measured the absorbance change at 448 nm in the time course for the CO rebinding to $P450_{nor}$ in a flash photolysis experiment (Figure 2). The kinetic trace was monophasic and fit well to a single-exponential function. On the basis of curve-fitting, the apparent first-order rate constant (k_{obs}) for reaction 2 was calculated. Under

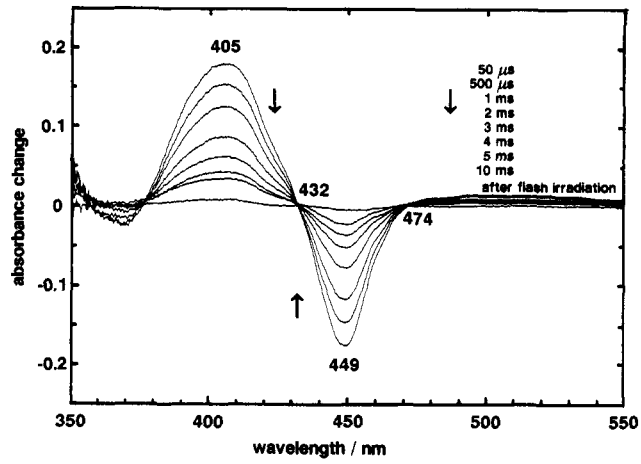

FIGURE 1: Difference spectral change of the CO complex of $P450_{nor}$ after laser irradiation. These spectra were based on the spectrum of the CO form of $P450_{nor}$, and recorded at 20 °C by multichannel photodiode array (UNISOKU, Osaka).

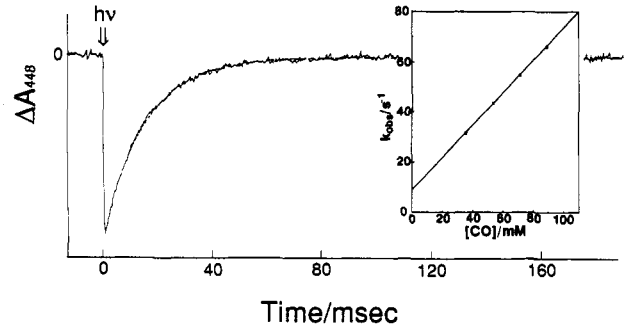

FIGURE 2: Time course of the absorbance change at 448 nm in CO rebinding to cytochrome $P450_{nor}$ on the flash photolysis experiment. The measurement condition employed was $[P450_{nor}CO] = 4$ μM in 0.1 M potassium phosphate buffer at pH 7.0 and 20 °C. The kinetic trace (solid line) fitted to a single-exponential function (dotted line) to yield the observed rate constant, k_{obs}, at an appropriate CO concentration. The *inset* shows the CO concentration dependence of k_{obs} under the pseudo-first-order condition ($[P450_{nor}] \ll [CO]$). From the slope and the y-intercept in this plot, we obtained the bimolecular association (k_{on}) and dissociation (k_{off}) rate constants in eq 2.

Table 1: Kinetic and Equilibrium Constants for the CO Binding Reaction at 20 °C, and IR Stretching of Iron-Bound CO for Cytochromes $P450_{nor}$ and $P450_{cam}$

	k_{on} ($\times 10^5$ M^{-1} s^{-1})	k_{off} (s^{-1})	K ($\times 10^4$ M^{-1})	ν_{CO} (cm^{-1})	$\Delta\nu_{1/2}$ (cm^{-1})
$P450_{nor}$	6.1	7.0	8.8	1942	20
$P450_{cam}(+)^a$	1.2	1.4	8.5	1940	13[b]
$P450_{cam}(-)^a$	140	6.4	222	1963	11[b]

[a] The kinetic and equilibrium constants for $P450_{cam}$ were referred from the paper by Iizuka et al. (1982). [b] O'Keeffe et al. (1978).

the pseudo-first-order condition ($[CO] \gg [P450_{nor}]$), a plot of the k_{obs} against the CO concentration employed gave a linear line, and then the association (k_{on}) and the dissociation (k_{off}) rate constants were estimated to be 6.1×10^5 M^{-1} s^{-1} and 7.0 s^{-1} from the slope and the y-intercept of this plot, respectively. We also estimated the equilibrium constant (K) from these data ($K = k_{on}/k_{off}$). In Table 1, the kinetic and equilibrium constants for $P450_{nor}$ are compiled and compared with those of $P450_{cam}$ reported previously (Iizuka et al., 1982; Peterson & Griffin, 1972). To check the reliability of our measurement for $P450_{nor}$, we also measured the kinetic and the equilibrium constants for $P450_{cam}(+)$ with the same apparatus. The kinetic data we obtained for $P450_{cam}(+)$ ($k_{on} = 0.7 \times 10^5$ M^{-1} s^{-1}, $k_{off} = 3.0$ s^{-1}, and $K = 2.2 \times 10^4$ M^{-1})

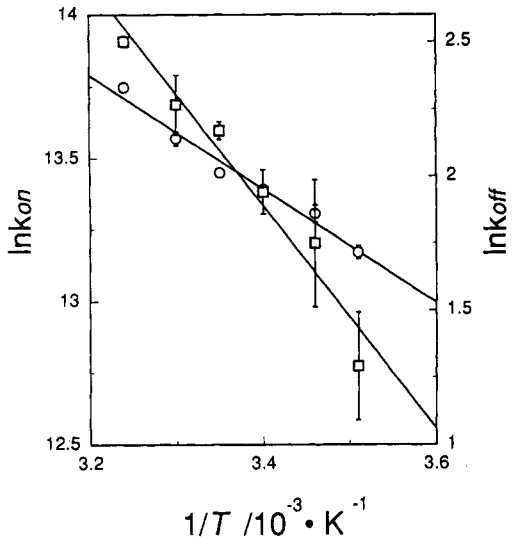

FIGURE 3: Arrhenius plots of k_{on} and k_{off} for cytochrome $P450_{nor}$. The logarithm of the k_{on} (○) and k_{off} (□) values at each temperature was plotted against the inverse of the absolute temperature. The enzyme was stable enough for the flash photolysis experiment at the temperature employed (11–36 °C).

were comparable to the published values. Comparing these values among the three P450s, the k_{on} value is increased in the order of $P450_{cam}(+)$, $P450_{nor}$, and $P450_{cam}(-)$, although the k_{off} value is the same magnitude for all of them. It is also noted that the equilibrium constant of $P450_{nor}$ is identical to that of $P450_{cam}(+)$ but smaller than that of $P450_{cam}(-)$.

We carried out the kinetic experiments and analyses for $P450_{nor}$ at various temperatures. The k_{on} and the k_{off} values obtained were plotted against $1/T$ (Arrhenius plot), which are illustrated in Figure 3. The plots show linearity in the temperature range measured. Values of the Arrhenius activation energy (E_a) and frequency factor (A) were obtained from the slope and the y-intercept in the Arrhenius plot, respectively. According to the transition state theory, we computed the activation and the difference values for the reaction profile of the CO-binding reaction (eq 2). The activation enthalpy $\Delta H^{\ddagger}$ and entropy $\Delta S^{\ddagger}$ were calculated from E_a and A, using the relationships $E_a = \Delta H^{\ddagger} + RT$ and $A = (ek_BT/h)\exp(\Delta S^{\ddagger}/R)$, where k_B and h are the Boltzmann and Planck constants, respectively. Values of $\Delta G^{\ddagger}$ were obtained from the equation $\Delta G^{\ddagger} = \Delta H^{\ddagger} - T\Delta S^{\ddagger}$. Finally, we determined the values of $\Delta G°$, $\Delta H°$, and $\Delta S°$ from the activation values.

The thermodynamic data obtained for $P450_{nor}$ are compared with the reported data for $P450_{cam}(+)$[2] and Mb in Table 2. The standard Gibbs energy ($\Delta G°$) shows a negative value for all samples, demonstrating the spontaneity of the CO-binding reaction for $P450_{nor}$ as well as $P450_{cam}(+)$ and Mb. When the Gibbs energy is divided into the enthalpy and entropy terms (Table 2), it was found that the $\Delta H°$ and $\Delta S°$ values are decreased in the order of $P450_{cam}(+)$, $P450_{nor}$, and Mb, suggesting that the stabilization of their CO complexes is controlled by different thermodynamic parameters. The CO complex of $P450_{cam}(+)$ is excessively stabilized by the entropy term (entropy dominant), while MbCO is stabilized by the enthalpy term rather than the entropy term (enthalpy dominant). For $P450_{nor}$CO, the $\Delta H°$ and $\Delta S°$ features are intermediate between those for $P450_{cam}(+)$ and Mb. This is also the case for comparison of the *off*-activation process; the $-\Delta S_{off}^{\ddagger}$ and $-\Delta H_{off}^{\ddagger}$ values are decreased in the same order as the $\Delta S°$ and $\Delta H°$ values. (Here, $-\Delta S_{off}^{\ddagger}$ and $-\Delta H_{off}^{\ddagger}$ mean the entropy and enthalpy changes from the transition to the CO-bound states.) In contrast, $\Delta S_{on}^{\ddagger}$ and $\Delta H_{on}^{\ddagger}$ are invariant among these hemoproteins. These characteristics of the thermodynamics in the CO-binding reaction may reflect the structural characteristics among the hemoproteins.

To gain insights into the structure of the CO-binding site, we measured the IR spectrum of the CO complex of $P450_{nor}$, where the iron-bound CO stretching band (ν_{CO}) is observed at 1942 cm^{-1} with a width at half-height ($\Delta\nu_{1/2}$) of 20 cm^{-1}, as shown in Figure 4. These values are compared with those of the CO complexes of $P450_{cam}$ in Table 1. The ν_{CO} value is somewhat different; $P450_{cam}(+) \cong P450_{nor} < P450_{cam}(-)$, and the $\Delta\nu_{1/2}$ value of $P450_{nor}$ is slightly larger than others, showing the structural difference in the Fe–C–O moiety among these P450s, which will be discussed in relation to the CO-binding properties.

DISCUSSION

For the first time, we obtained the kinetic (k_{on} and k_{off}), the equilibrium (K), and the thermodynamic (ΔG, ΔS, and ΔH) parameters in the CO-binding reaction, and the IR stretching band for the iron-bound CO (ν_{CO}) for $P450_{nor}$. Comparing these values with those of $P450_{cam}$, we can reveal the structural characteristics of $P450_{nor}$ responsible for the CO-binding reaction, which are possibly correlated with its unique catalytic property.

Kinetics and Equilibrium in CO Binding. Recently, several pieces of structural information for $P450_{nor}$ have been accumulated. Some spectroscopic results are consistent with the ligation of the thiolate anion of Cys as a fifth axial ligand, and a vacancy at the sixth site in the ferrous high-spin form (Nakahara et al., 1993). Primary structure alignment between $P450_{nor}$ and $P450_{cam}$ (Kizawa et al., 1991) showed that the amino acid residues interacting with the heme are highly conserved. Thus, it seems reasonable to suggest that the structure of the iron ligands in $P450_{nor}$ is similar to that of $P450_{cam}$, so that the difference in the kinetics and the equilibrium reaction in CO binding between $P450_{nor}$ and $P450_{cam}$ (see Table 1) is attributable to differences in the protein structure in the heme environment.

It is generally accepted that in the binding of ligands to hemoproteins, local polarity, steric hindrance, and hydrogen bonding in the heme pocket influence the kinetic and equilibrium features. For example, the effect of point-mutation on ligand binding to Mb has been explained in terms of these contributions (Springer et al., 1989; Cameron et al., 1993; Quillin et al., 1993). In particular, the steric effect on the CO ligand, which is exerted by the distal amino acid residues, is suggested to be most important in CO binding to hemoproteins, as has been manifested in the model studies (Springer et al., 1989). In the case of $P450_{cam}$, the slower on-rate and the lower affinity of CO in $P450_{cam}(+)$ than those in $P450_{cam}(-)$ have been readily interpreted in terms of the steric hindrance to the CO ligand by the bound camphor, in good agreement with X-ray crystallographic (Raag & Poulos, 1989b) and IR studies (O'Keefe et al., 1978).

Similarly, our present results, where the kinetic and equilibrium data of $P450_{nor}$ are different from those of $P450_{cam}(+)$ and $P450_{cam}(-)$ (Table 1), likely reflect differences in the steric hindrance in the CO association to the heme iron. The k_{on} feature [$P450_{cam}(+) < P450_{nor} < P450_{cam}(-)$] showed that CO binding to $P450_{nor}$ is sterically less restricted than to $P450_{cam}(+)$ but not as free as to $P450_{cam}(-)$. This fact implies that the ligand pathway and/or the heme pocket of $P450_{nor}$

[2] Kato, M., Makino, R., & Iizuka, T. (1994) *Biochim. Biophys. Acta* (in press).

Table 2: Thermodynamic Parameters for the CO Binding Reaction by Cytochromes $P450_{nor}$ and $P450_{cam}(+)$ and Myoglobin at 25 °C

	$\Delta G_{on}^{\ddagger}$ (kcal mol^{-1})	$\Delta G_{off}^{\ddagger}$ (kcal mol^{-1})	$\Delta H_{on}^{\ddagger}$ (kcal mol^{-1})	$\Delta H_{off}^{\ddagger}$ (kcal mol^{-1})	$\Delta S_{on}^{\ddagger}$ (cal K^{-1} mol^{-1})	$\Delta S_{off}^{\ddagger}$ (cal K^{-1} mol^{-1})	$\Delta G°$ (kcal mol^{-1})	$\Delta H°$ (kcal mol^{-1})	$\Delta S°$ (cal K^{-1} mol^{-1})
$P450_{nor}$	9.5	16.2	3.2	7.7	−21.0	−28.7	−6.7	−4.4	7.7
$P450_{cam}(+)$[a]	10.7	16.8	7.0	2.9	−12.4	−46.6	−6.1	4.1	34.2
Mb[b]	9.8[c]	19.2[d]	4.1[c]	14.8[d]	−19.4[c]	−15[d]	−9.4[e]	−10.7[e]	−4.8[e]

[a] The data for $P450_{cam}(+)$ were referred from the paper by Kato et al. (see footnote 2). [b] Sperm whale myoglobin. [c] Hasinoff (1974). [d] Projahn & Eldik (1991). [e] Thermodynamic values in the equilibrium were calculated on the basis of the kinetic data reported previously.

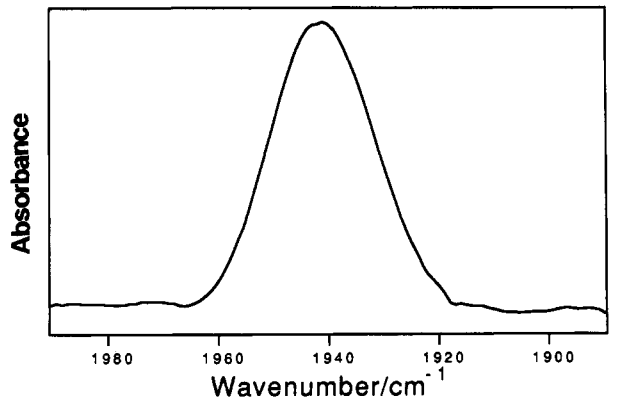

FIGURE 4: Absorption of iron-bound CO stretching in the IR spectrum of the CO complex for cytochrome $P450_{nor}$. The CO stretching was observed at 1942 cm^{-1}. CaF_2 was used as a cell window, and the path length was 0.050 mm.

is more widely opened than that of $P450_{cam}(+)$, or the protein conformation of $P450_{nor}$ changes for the CO ligand to have easier access to the heme iron than that in $P450_{cam}(+)$. However, the second possibility, i.e., large conformational changes during CO association, would be ruled out on the basis of the thermodynamic study, discussed in the following section (*vide infra*).

In this respect, it is also interesting to find that iron-bound CO stretching is observed at 1942 cm^{-1} for $P450_{nor}CO$ (see Figure 4). The band position is almost identical to that for $P450_{cam}(+)CO$ but smaller than that for $P450_{cam}(-)CO$, showing that the Fe–C–O structure (e.g., bond angle, length, etc.) in $P450_{nor}$ is very similar to that in $P450_{cam}(+)$, but somewhat different from that in $P450_{cam}(-)$, assuming that the $Fe-S^-$ character is similar in all of them. In other words, the Fe–C–O bond in $P450_{nor}$ is sterically constrained by the surrounding amino acid residues in its heme distal pocket to the same extent as that by the bound camphor in $P450_{cam}(+)$. This suggestion seemed to be supported by the equilibrium data (see Table 1), where the K value of $P450_{nor}$ is almost the same as that of $P450_{cam}(+)$. The IR data show the same size of the heme pocket immediate to the CO-binding site in $P450_{nor}$ as that in $P450_{cam}(+)$. Thus, combining the IR result with the kinetic data, we could suggest that the heme pocket size is almost the same, but the channel in $P450_{nor}$ for ligand entry from the solvent region to the heme pocket is sterically less restricted (i.e., the open channel) than that of $P450_{cam}(+)$.

Recently, Ravichandran et al. (1993) reported the crystal structure of the hemoprotein domain of $P450_{BM3}$. In spite of low sequence identity in the primary structure, the three-dimensional structure of $P450_{BM3}$ is very similar to that of $P450_{cam}$. This fact allows us to suggest that the heme pocket structure of $P450_{nor}$ would be basically the same as those of any other P450s. However, on the basis of the present IR data, we can suggest that the position of the distal residues relative to the heme in $P450_{nor}$ is somewhat different from that in $P450_{cam}$; although the CO stretching band is located at the same position, the steric constraint in $P450_{cam}(+)$ is predominantly exerted by the bound camphor, while $P450_{nor}$ does not have any substrate-binding site. This structural characteristic at the heme distal pocket may be relevant to the difference in the CO-binding property and further in their catalytic properties.

Thermodynamics of CO Binding. In comparing the thermodynamic parameters in the CO-binding reaction between $P450_{nor}$, $P450_{cam}(+)$, and Mb, the most remarkable feature is the entropy changes in the equilibrium and the *off*-activation processes (see Table 2). We cannot so easily discuss the $\Delta S°$ in the equilibrium process in detailed structural terms, because it involves many structural contributions. However, we can speculate that the difference in $\Delta S°$ among the hemoproteins comes from the difference in the change in the weak intramolecular interactions in the protein such as hydrogen bonding, Coulombic force, van der Waals contact, and so on, in going from the CO-free to the CO-bound states, because the entropy change is generally indicative of the change in the freedom in the system from the initial to the final states. Concerning the changes in the weak intramolecular interactions in the protein, it would be endothermic processes when releasing constraint of internal rotation and vibrations of molecular fragments in the protein. Indeed, the $\Delta H°$ is increased in the same order [Mb < $P450_{nor}$ < $P450_{cam}(+)$] as the $\Delta S°$. This enthalpy feature supports the general idea that the change in the weak intramolecular interaction in the protein is reflected in the entropy change in the CO-binding reaction. The large positive value of $\Delta S°$ in $P450_{cam}(+)$ means that these intramolecular weak bonds are broken and/or loosened upon CO binding. By contrast, its small value in $P450_{nor}$ shows that these intramolecular bonds are almost maintained between the CO-free and the CO-bound forms.

It is more difficult to discuss the thermodynamics in the activation processes, because the transition state cannot be definitively identified in CO binding to $P450_{nor}$. However, it is worthwhile to note that the order of the $-\Delta S_{off}^{\ddagger}$ values is the same as that of the $\Delta S°$ values, and is also the same as that of $-\Delta H_{off}^{\ddagger}$. In the above discussion for $\Delta S°$, the observation likely indicates that the $-\Delta S_{off}^{\ddagger}$ corresponds to the magnitude of the change in the weak intramolecular interactions in the protein from the transition to the CO-bound states, which is increased in the order of Mb, $P450_{nor}$, and $P450_{cam}(+)$. These thermodynamic features in the equilibrium and the *off*-activation processes are possibly correlated with their structural characteristics and/or functional properties. For example, in the case of Mb, an increase in the entropy is rather unsuitable for stabilization of the iron-bound O_2, because it would increase the probability of attack of water molecules on the $Fe-O_2$ moiety, resulting in fast autoxidation.

One possible explanation for the difference in the thermodynamic features between $P450_{cam}(+)$ and $P450_{nor}$ arises from the difference in substrate binding. $P450_{cam}(+)$ has a noncovalently bound camphor at its active site. The crystal structure of the $P450_{cam}(+)CO$ ternary complex has shown

that the camphor moves slightly from the position in the ferric enzyme and its temperature factors also increase upon CO binding (Raag & Poulos, 1989b). These changes could contribute to the large entropy change in each process. However, $P450_{nor}$ is not supposed to have a substrate-binding site in its heme pocket. In contrast to $P450_{cam}$, this structural characteristic of $P450_{nor}$ is reasonably consistent with the smaller entropy change upon CO binding.

Another one is based on the difference in the catalytic reaction between $P450_{nor}$ and $P450_{cam}$. In the catalytic cycle of $P450_{cam}$, the enzyme forms a ternary complex with the substrate *d*-camphor and O_2, and it further interacts with another protein, the reductase, to accept electrons for O–O bond cleavage (Hinz & Peterson, 1981; Hinz et al., 1982). The turnover of this catalytic cycle is 25 s^{-1} (Makino et al., 1982). In contrast, the reaction catalyzed by $P450_{nor}$ (eq 1) is less complex than the monooxygenation and much faster (more than 500 s^{-1} for its turnover) (Nakahara et al., 1993). During the reaction, $P450_{nor}$ does not need substrate and reductase binding but binds with only NADH as an electron donor. This fact allows us to imagine that the protein structure of $P450_{nor}$ changes less drastically during the catalytic reaction than that of $P450_{cam}$. Thus, such a difference in the protein dynamics could explain the difference in the thermodynamics between $P450_{nor}$ and $P450_{cam}(+)$.

In conclusion, we found that the heme distal pocket of $P450_{nor}$ has the same size as that of $P450_{cam}(+)$, but its channel from the solvent phase to the heme pocket is relatively opened to allow easy access for external ligands, compared with that of the $P450_{cam}(+)$. The protein conformation of $P450_{nor}$ may change upon CO binding less than that of $P450_{cam}$, resulting in the slight entropy change. Since this enzyme does not have a substrate-binding site, this structural characteristic at the active site may be also reflected in the thermodynamics. These features are well consistent with the unique catalytic reaction of $P450_{nor}$: very rapid NO reduction to N_2O. We are now characterizing the heme environmental structure of $P450_{nor}$ using some spectroscopic methods such as ESR, NMR, and Raman spectroscopies. Finally, we have obtained single crystals (Nakahara et al., 1994) and have initiated the X-ray crystallographic structure determination.

ACKNOWLEDGMENT

We thank Prof. R. Makino (Himeji Institute of Technology) for his kind gift of $P450_{cam}$, and Dr. T. Noguchi (RIKEN, Solar Energy Group) for his help in the IR measurements.

REFERENCES

Cameron, A. D., Smerdon, S. J., Wilkins, A. J., Habash, J., Helliwell, J. R., Li, T., & Olson, J. S. (1993) *Biochemistry 32*, 13061–13070.

Gunsalus, I. C., Meeks, J. R., Lipscomb, J. D., Debrunner, P., & Munck, E. (1974) in *Molecular Mechanism of Oxygen Activation* (Hayaishi, O., Ed.) pp 559–613, Academic Press, New York.

Hasinoff, B. B. (1974) *Biochemistry 13*, 3111–3117.

Hinz, M. J., & Peterson, J. A. (1981) *J. Biol. Chem. 256*, 6721–6728.

Hinz, M. J., Mock, D. M., Peterson, L. L., Tuttle, K., & Peterson, J. A. (1982) *J. Biol. Chem. 257*, 14324–14332.

Iizuka, T., Watanabe, K., Makino, R., Sakaguchi, K., Mitani, F., Ishimura, Y., Kawabe, K., Yoshida, Z., & Ogoshi, H. (1982) in *Oxygenase and Oxygen Metabolism* (Nozaki, M., Yamamoto, S., Ishimura, Y., Coon, M. J., Ernster, L., & Estabrook, R. W., Eds.) pp 445–450, Academic Press, New York.

Kizawa, H., Tomura, D., Oda, M., Fukumuzu, A., Hoshino, T., Gotoh, O., Yasui, T., & Shoun, H. (1991) *J. Biol. Chem. 266*, 10632–10637.

Makino, R., Iizuka, T., Sakaguchi, K., & Ishimura, Y. (1982) in *Oxygenase and Oxygen Metabolism* (Nozaki, M., Yamamoto, S., Ishimura, Y., Coon, M. J., Ernster, L., & Estabrook, R. W., Eds.) pp 467–477, Academic Press, New York.

Nakahara, K., Tanimoto, T., Hatano, K., Usuda, K., & Shoun, H. (1993) *J. Biol. Chem. 268*, 8350–8355.

Nakahara, K., Shoun, H., Adachi, S., Iizuka, T., & Shiro, Y. (1994) *J. Mol. Biol. 239*, 158–159.

O'Keefe, D. H., Eble, R. E., Peterson, J. A., Maxwell, J. C., & Caughey, W. S. (1978) *Biochemistry 17*, 5845–5852.

Omura, T., & Sato, R. (1962) *J. Biol. Chem. 237*, 1375–1376.

Peterson, J. A., & Griffin, B. W. (1972) *Arch. Biochem. Biophys. 151*, 427–433.

Poulos, T. L., & Howard, A. J. (1987) *Biochemistry 26*, 8165–8174.

Poulos, T. L., Finzel, B. C., Gunsalus, I. C., Wagner, G. C., & Kraut, J. (1985) *J. Biol. Chem. 260*, 16122–16130.

Poulos, T. L., Finzel, B. C., & Howard, A. J. (1986) *Biochemistry 25*, 5314–5322.

Poulos, T. L., Finzel, B. C., & Howard, A. J. (1987) *J. Mol. Biol. 195*, 687–700.

Projahn, H.-D., & Eldik, R. (1991) *Inorg. Chem. 30*, 3288–3293.

Quillin, M. L., Arduini, R. M., Olson, J. S., & Phillips, G. N., Jr. (1993) *J. Mol. Biol. 234*, 140–155.

Raag, R., & Poulos, T. L. (1989a) *Biochemistry 28*, 917–922.

Raag, R., & Poulos, T. L. (1989b) *Biochemistry 28*, 7586–7592.

Ravichandran, K. G., Boddupalli, S. S., Hasemann, C. A., Peterson, J. A., & Deisenhofer, J. (1993) *Science 261*, 731–736.

Sato, F., Shiro, Y., Sakaguchi, Y., Iizuka, T., & Hayashi, H. (1990a) *J. Biol. Chem. 265*, 18823–18828.

Sato, F., Shiro, Y., Sakaguchi, Y., Suzuki, T., Iizuka, T., & Hayashi, H. (1990b) *J. Biol. Chem. 265*, 2004–2010.

Shoun, H., & Tanimoto, T. (1991) *J. Biol. Chem. 266*, 11078–11082.

Shoun, H., Sudo, Y., Seto, Y., & Beppu, T. (1983) *J. Biochem. 94*, 1219–1229.

Shoun, H., Suyama, W., & Yasui, T. (1989) *FEBS Lett. 244*, 11–14.

Sligar, S. G., & Murray, R. I. (1986) in *Cytochrome P-450* (Ortiz de Montellano, P. R., Ed.) pp 429–503, Plenum, New York.

Springer, B. A., Egeberg, K. D., Sligar, S. G., Rohlfs, R. J., Mathews, A. J., & Olson, J. S. (1989) *J. Biol. Chem. 264*, 3057–3060.